HHS Public Access

Author manuscript

Cell. Author manuscript; available in PMC 2016 December 17.

Published in final edited form as:

Cell. 2015 December 17; 163(7): 1742–1755. doi:10.1016/j.cell.2015.11.019.

Coordinated and Compartmentalized Neuromodulation Shapes Sensory Processing in *Drosophila*

Raphael Cohn[1], **Ianessa Morantte**[1], and **Vanessa Ruta**[1,*]

[1]Laboratory of Neurophysiology and Behavior, The Rockefeller University, New York, NY 10065, USA

SUMMARY

Learned and adaptive behaviors rely on neural circuits that flexibly couple the same sensory input to alternative output pathways. Here, we show that the *Drosophila* mushroom body functions like a switchboard in which neuromodulation reroutes the same odor signal to different behavioral circuits, depending on the state and experience of the fly. Using functional synaptic imaging and electrophysiology, we reveal that dopaminergic inputs to the mushroom body modulate synaptic transmission with exquisite spatial specificity, allowing individual neurons to differentially convey olfactory signals to each of their postsynaptic targets. Moreover, we show that the dopaminergic neurons function as an interconnected network, encoding information about both an animal's external context and internal state to coordinate synaptic plasticity throughout the mushroom body. Our data suggest a general circuit mechanism for behavioral flexibility in which neuromodulatory networks act with synaptic precision to transform a single sensory input into different patterns of output activity.

Graphical Abstract

*Correspondence: ruta@rockefeller.edu.

AUTHOR CONTRIBUTIONS

R.C. and V.R. conceived the project and wrote the paper. R.C. performed all experiments and data analysis, except Figures 5E, S1G, S4B, S5B, and S5E, which were carried out by I.M.

SUPPLEMENTAL INFORMATION

Supplemental Information includes Supplemental Experimental Procedures, seven figures, one table, and three movies and can be found with this article online at http://dx.doi.org/10.1016/j.cell.2015.11.019.

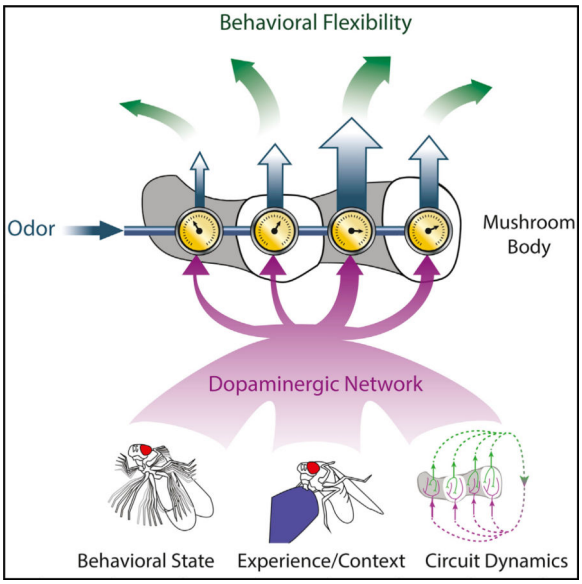

INTRODUCTION

Animals must constantly adapt their behavior to meet the demands of their ever-changing external environment and internal needs. Neuromodulators provide an evolutionarily conserved mechanism to generate behavioral variability (Bargmann, 2012; Marder, 2012). By rapidly regulating neuronal excitability and the strength of synaptic connections between neurons, neuro-modulators confer functional flexibility to anatomically invariant circuits. Context- and state-dependent patterns of neuromodulator release can thereby tune neural circuit properties to produce alternative responses to the same sensory stimulus.

Dopaminergic pathways have been investigated extensively as part of a reinforcement system that motivates and modifies many facets of animal behavior (Beninger, 1983; Bromberg-Martin et al., 2010; Redgrave and Gurney, 2006; Schultz et al., 1997; Waddell, 2013; Wise, 2004). Dopamine acts through multiple receptors that couple to distinct intracellular signaling cascades, enabling this single neuromodulator to have diverse effects on synaptic function and communication (Tritsch and Sabatini, 2012). Linking mechanisms of synaptic modulation to the generation of adaptive behaviors, however, requires a circuit-level understanding of how dopaminergic pathways encode the ongoing experience of an animal and reinforce appropriate neural circuit configurations. While mammalian midbrain dopaminergic neurons are known to be important mediators of flexible circuit processing, their anatomic and functional heterogeneity and the intricate wiring of their target neuropils (Beier et al., 2015; Fiorillo et al., 2013; Lammel et al., 2014; Lerner et al., 2015) have made it difficult to resolve how they can selectively alter synaptic signaling between different neural pathways. Moreover, the dopamine they release has been suggested to act over long distances, by diffusing through the extracellular space, and at select synaptic sites (Rice et al., 2011). Consequently, how dopaminergic pathways sculpt synaptic connections to precisely shape circuit function remains unclear.

The insect mushroom body is an integrative brain center whose orderly circuit architecture provides an opportunity to examine how neuromodulators flexibly regulate the flow of sensory information. In *Drosophila*, the mushroom body has been best studied for its essential role in olfactory learning in which past experience alters the subsequent behavioral response to an odor (Heisenberg, 2003; Keene and Waddell, 2007). The convergence of olfactory and dopaminergic reinforcement signals in the mushroom body also renders it ideally suited to shape odor processing based on the acute needs of an animal. Indeed, the mushroom body plays a role in the context-dependent processing of odor signals, modulating innate olfactory preferences in response to ongoing changes to a fly's environment or internal state (Lewis et al., 2015; Owald et al., 2015).

In the mushroom body, odors are encoded as sparse ensembles of activated Kenyon cells (KCs) (Campbell et al., 2013), each of which integrates input from diverse combinations of olfactory glomeruli in the calyx (Caron et al., 2013; Gruntman and Turner, 2013). The ~2,000 KCs propagate their odor responses along parallel axon fibers into the mushroom body's output lobes. Here we focus on γ KCs, each of which projects a single axon that traverses across the γ lobe (Figures 1A and 1B). Each KC axon synapses onto a small number of mushroom body output neurons (MBONs), whose segregated dendrites tile the complete length of the lobe to form five discrete anatomic compartments (γ1–γ5) (Figures 1A and 1C). The MBONs, as the only known efferent pathways of the mushroom body, must translate KC odor representations into adaptive behavioral responses (Aso et al., 2014a; Tanaka et al., 2008). MBON axons converge on a small number of target neuropils, where their concerted activity has been proposed to bias an animal's innate and learned olfactory preferences (Aso et al., 2014b; Hige et al., 2015; Owald et al., 2015).

The mushroom body lobes are also richly innervated by dopaminergic neurons (DANs) thought to convey the contextual signals that impart meaning to an odor (Aso et al., 2012; Burke et al., 2012; Claridge-Chang et al., 2009; Liu et al., 2012; Mao and Davis, 2009; Waddell, 2013; Yamagata et al., 2015). Rewarding and punishing experiences have been shown to activate distinct subsets of DANs, each of which projects axons into just one of the lobe compartments (Figures 1A and 1D), mirroring the segregated innervation pattern of the MBONs. This anatomic arrangement suggests that DANs may convey positive and negative contextual information to different synapses along a KC axon, permitting differential tuning of neurotransmission to each MBON under different circumstances.

Here we took advantage of the mushroom body's anatomic organization to elucidate how dopaminergic pathways instruct synaptic and circuit plasticity. We developed a synaptic activity reporter to visualize spatiotemporal patterns of modulation, and we demonstrate that DANs modify synapses in discrete subcellular domains along the length of individual KC axons. Moreover, we show that DANs form part of a highly interconnected network that coordinates synaptic plasticity across the mushroom body in response to both external contextual cues and the fly's internal state. Thus, the concerted action of the dopaminergic population acts with exquisite spatial precision to regulate the flow of olfactory signals to each mushroom body output pathway, providing a circuit mechanism to generate flexible responses to an odor.

RESULTS

An Optical Sensor of Presynaptic Activity

Presynaptic Ca^{2+} is a key regulator of neurotransmission and effector of neuromodulation (Regehr, 2012), suggesting it should provide a sensitive readout of synaptic function. We therefore generated sytGCaMP, in which the genetically encoded Ca^{2+} indicator GCaMP6s is tethered to the C terminus of the vesicular synaptic protein synaptotagmin (Figure S1A). We initially confirmed that sytGCaMP co-localizes with endogenous synaptic proteins and consequently detects Ca^{2+} influx specifically at presynaptic terminals (Figures S1B–S1G). We then expressed sytGCaMP in all γ KCs using a selective promoter (Figure S1H), and we focally stimulated the calyx to activate an individual neuron in a brain explant. We performed volumetric two-photon imaging to capture the fluorescently tagged synapses of the KC's full axonal arbor as it ramified through multiple imaging planes within the γ lobe. Stimulation of a single KC evoked robust fluorescence increases at punctate loci distributed along the length of its axon (Figures 1E and S1I), consistent with sytGCaMP's synaptic localization and anatomic evidence that KCs form output synapses in all compartments of the γ lobe (Figures S1J and S4B). Thus, sytGCaMP facilitates the detection of Ca^{2+} influx at individual synaptic sites, providing a technical strategy to resolve differences in presynaptic function and modulation across the compartments of the lobe.

DANs Represent Context through Coordinated Patterns of Activity

We next used the presynaptic localization of sytGCaMP to monitor the activity of the DAN population and gain insight into the patterns of dopamine release across the γ lobe in different contexts. We combined the tyrosine hydroxylase and dopa-decarboxylase promoters to drive expression of sytGCaMP in the DANs, innervating every compartment of the γ lobe. The axon terminals of DANs innervating the γ2–γ5 compartments could be monitored in a single optical imaging plane, allowing us to simultaneously record their synaptic responses to positive and negative reinforcement stimuli (Figure 2A).

Discrete subsets of DANs are sufficient to instruct learned odor attraction or aversion, suggesting they may autonomously encode the contextual signals that impart meaning to an olfactory experience. However, while sugar feeding activated the γ4 and γ5 DANs, in accord with their established role in driving the formation of appetitive olfactory associations (Liu et al., 2012; Yamagata et al., 2015; Waddell, 2013), we observed that sucrose ingestion also inhibited the γ2 and γ3 DANs (Figure 2B; Movie S1; Table S1). Conversely, the γ2 DAN has been shown to respond to electric shock and contribute to aversive olfactory conditioning (Aso et al., 2012; Claridge-Chang et al., 2009; Mao and Davis, 2009). We confirmed that a brief electric shock applied to the fly's abdomen activated the γ2 DAN, but found that it also excited the γ3 DANs and inhibited the γ4 and γ5 DANs (Figure 2C). Thus, the DANs of each compartment represent reinforcement stimuli through either excitation or inhibition, analogous to the bidirectional signaling observed in mammalian midbrain DANs in response to positive and negative cues (Bromberg-Martin et al., 2010; Lerner et al., 2015). The reciprocal patterns of DAN activity evoked by these appetitive and aversive stimuli suggest that mushroom body reinforcement pathways may act in concert to regulate olfactory processing through coordinated patterns of dopamine release across compartments.

DAN activity fluctuated significantly even in the absence of overt stimulation. Video monitoring of the fly during DAN imaging revealed that these fluctuations are highly correlated with motor output (Figure 2D; Movie S2). Tethered animals generally alternated between two distinct behavioral states—quiescence and rapid kicking or flailing that resembled escape behavior. Flailing was strongly correlated with high γ2/γ3 and low γ4/γ5 DAN activity, similar to the pattern evoked by electric shock. In contrast, quiescence elicited the reciprocal pattern, resembling the DAN response to sugar feeding (Figures 2E and S2A). Thus, different behavioral states induce distinct bidirectional patterns of activity across the DAN population. Interestingly, the strict correlations exhibited by DANs during tethered behavior were altered when the same fly walked on a freely rotating ball (Figure S2B). For example, during walking, γ4 and γ5 DANs were no longer strictly synchronized and γ4 DANs instead became transiently entrained to either γ3 or γ5 DAN activity. Odor stimuli, likewise, disrupted the baseline correlations between DANs (Figure S2C). These observations imply that the functional relationships between DANs are not absolute but rather an emergent property, depending on both salient external sensory signals and a fly's internal state.

Functional Communication between Compartments Coordinates DAN Activity

Recent anatomic data reveal that DANs and MBONs innervating different compartments may be functionally interconnected via overlapping projections in the protocerebrum (Aso et al., 2014a). We therefore asked whether the correlated, partially antagonistic DAN activity patterns we observed are shaped by circuit interactions between compartments. We used the 58E02 promoter fragment (Liu et al., 2012) to selectively express the ATP-gated $P2X_2$ channel in a subset of DANs, including those innervating the γ4 and γ5 compartments. Activation of 58E02+ DANs by application of ATP to their dendrites evoked robust inhibition of the γ2 DAN (Figure 3A). The γ3 DANs also frequently were inhibited but occasionally activated, due to variable labeling of this compartment by the 58E02 driver. Therefore, excitation of a subset of DANs is sufficient to suppress those targeting other compartments, yielding a bidirectional pattern of activity similar to that evoked by a sugar reward. Direct or indirect communication between the DANs innervating different compartments may, therefore, underlie their concerted representation of reinforcement signaling.

To investigate whether feedback from MBONs contributes to the functional coordination of DANs, we stimulated individual γ MBONs using sparse driver lines to express $P2X_2$ and focally injecting ATP onto their axons. Activation of each γ lobe MBON triggered excitation or inhibition of the DANs in every compartment (Figures 3B–3E), similar to the distributed activity patterns evoked by physiological reinforcement experiences. The bidirectional nature of DAN activity elicited by excitation of single MBONs indicates that multisynaptic interactions functionally link extrinsic neurons innervating different compartments. Thus, MBONs and DANs comprise a complex interconnected network, providing a potential substrate for the diverse functional relationships between DANs that emerge in different behavioral contexts (Figures 2 and S2). Together, these data suggest that DANs do not act autonomously to convey the valence of a reinforcement stimulus to just a single compartment, but rather they function as a dynamic ensemble, integrating information

about environmental stimuli and internal state to convey the moment-by-moment experience of the fly to all compartments of the lobe.

Compartmentalized Synaptic Domains along KC Axons

We next asked how coordinated patterns of DAN activity might shape the flow of olfactory signals along KC axons as they traverse through the different compartments of the lobe. We expressed sytGCaMP in γ KCs (Figure 4A) and used volumetric two-photon imaging to monitor their complement of synapses within the γ lobe in vivo. Unexpectedly, the distribution of odor-evoked presynaptic Ca^{2+} along KC axons was highly non-uniform and displayed a discrete modular organization in each of the 12–18 imaging planes (Figures 4B, 4C, S3A, S3B, and S4C; Movie S3). The asymmetry in presynaptic Ca^{2+} was often apparent basally, prior to odor stimulation (Figure S3D), suggesting that persistent differences in synaptic function along KC axons could influence the processing of all incoming odor stimuli. Consistent with this idea, the same modular pattern of presynaptic Ca^{2+} was evoked in response to every odor tested and over a range of concentrations (Figures S3E and S4H).

Alignment of sytGCaMP responses with the projections of MBONs and DANs in the γ lobe indicated that the discrete Ca^{2+} domains apparent in KC axons map to the different compartments of the lobe (Figure S3F). To confirm this, we imaged KC synaptic responses in animals that also expressed a red fluorophore in a subset of DANs, and we observed that the sharp borders separating regions of high and low synaptic Ca^{2+} aligned with the compartmental boundaries (Figure 4E). Odor-evoked synaptic responses in KCs were significantly more robust in the γ2 and γ3 compartments relative to those in the γ4 compartment, with even weaker responses evident in the γ5 compartment (Figure 4C). Thus, the distribution of presynaptic Ca^{2+} along KC axons adheres to the modular architecture of the lobes, demonstrating that the anatomic compartments represent functionally distinct units. Moreover, KC classes innervating other lobes also exhibited modular sytGCaMP signals (Figure S3G), indicating that compartmentalized synaptic Ca^{2+} is a general feature of odor representations in the mushroom body lobes.

Asymmetric presynaptic Ca^{2+} domains could arise from differences in KC innervation along the γ lobe or from functional variation along individual KC axons. Single-cell labeling of >80 γ KCs verified they invariantly traverse the entire lobe (Figure S4A) and are poised to carry the same odor signals to each compartment. However, functional synaptic heterogeneity was evident along sparsely labeled KC axons (Figures 4F and S3C) co-expressing sytGCaMP and a red fluorophore to delineate their anatomic projections. Synaptic boutons decorating the same KC axons exhibited differential responses to odor, with more robust activity evoked in the individual synapses in the γ2 and γ3 compartments relative to those in the γ4 and γ5 compartments. Although we did not routinely image the γ1 compartment, presynaptic Ca^{2+} was often lower there in comparison to more distal portions of the lobe (Figure 4C), indicating it is unlikely that action potentials simply fail to propagate the length of KC axons. Together, these data suggest that synapses along individual KC axons are functionally diverse, such that the same olfactory signal is differentially represented by each axonal segment of a neuron.

Dopamine Modulates Synapses along KC Axons

The asymmetry of KC synaptic responses points to the possibility that active modulation by the DANs that tile the γ lobe may regulate synaptic signaling within each compartment. Interestingly, while DAN activity patterns rapidly fluctuated in tethered animals, the high γ2/γ3 and low γ4/γ5 DAN network state significantly predominated (Figure S2D), potentially reflecting a fly's frequent struggle to escape. The similarity between this DAN network state (Figure 2E) and the pattern of KC presynaptic Ca^{2+} we consistently observed (high γ2/γ3 and low γ4/γ5, Figure 4C) led us to ask if the behavioral state of the fly can directly modulate olfactory signaling along the lobe. We therefore examined KC responses in a brain explant where basal fluctuations in DAN activity were greatly reduced (data not shown), and we found that direct activation of KCs evoked a uniform sytGCaMP signal across the length of the lobe in this ex vivo preparation (Figures 4D, S4D, and S4E). In contrast, direct KC stimulation in vivo elicited a modular response pattern (Figures S4F and S4G) resembling that triggered by odor. We therefore conclude that, while KC axons have the anatomic potential to transmit equivalent neural signals to all compartments of the γ lobe, in vivo modulation induces functional heterogeneity along their length.

We next asked whether acute alterations to the state or circumstances of an animal can modify the pattern of presynaptic Ca^{2+} along KCs. Given that sucrose ingestion elicits the reciprocal pattern of DAN activity (high γ4/γ5 and low γ2/γ3, Figure 2B) as that associated with flailing behavior, we reasoned this appetitive reward might alter the distribution of presynaptic Ca^{2+} across lobe compartments. Overnight fasting did not change the profile of presynaptic Ca^{2+} along γ KCs (Figure S3E). However, after sugar feeding the odor-evoked synaptic responses in the γ4 and γ5 compartments relatively increased, while the responses in the γ2 compartment relatively decreased (Figure 5A). Sucrose ingestion, therefore, differentially modulates the olfactory responses of KC synapses along the γ lobe, paralleling the bidirectional pattern of DAN activity evoked by this appetitive reward.

To confirm that DAN activation is sufficient to modify odor-evoked synaptic responses in KCs, we used the 58E02 promoter to drive expression of $P2X_2$ in the γ4 and γ5 DANs excited by sugar feeding (Figure 2B). Stimulation of 58E02+ DANs with ATP altered the profile of odor-evoked Ca^{2+} along γ KC axons, relatively increasing the signal in the distal lobe compartments while decreasing it in the proximal compartments (Figures 5B and 5C), resembling the changes induced by sucrose ingestion. Thus, both exogenous and physiological activation of DAN reinforcement pathways can modulate KC synapses with striking spatial precision. Changes in odor-evoked presynaptic Ca^{2+} persisted for the duration of an experiment (up to ~1 hr, Figure S5A), indicating that intensely salient experiences, like tethering or sugar ingestion, can alter the state of KC synapses with enduring consequences for how all subsequent olfactory signals are processed.

Dopamine receptors DopR1 and DopR2 are both highly expressed within the mushroom body lobes and comprise essential molecular pathways regulating the formation and maintenance of learned olfactory associations (Berry et al., 2012; Kim et al., 2007; Qin et al., 2012). To verify that dopaminergic signaling directly contributes to compartmentalized patterns of synaptic modulation along KCs, we examined mutants for these receptors and

found that the profile of odor-evoked sytGCaMP fluorescence was inverted in *DopR2* mutants (Figure 5D). Selective knockdown of *DopR2* in γ KCs using RNAi similarly altered the pattern of synaptic Ca^{2+} along KC axons (Figures 5E and S5B), demonstrating that dopamine acts presynaptically to shape odor processing.

DopR1 mutants exhibited a subtler phenotype (Figure S5C), while the distribution of synaptic Ca^{2+} in *DopR1*/*DopR2* double mutants was still asymmetric (Figure S5D), implying that additional dopamine receptors or neuromodulatory pathways (Aso et al., 2014a; Tanaka et al., 2008) may influence the patterning of KC presynaptic Ca^{2+}. We therefore examined synaptic responses in mutants for the dopamine reuptake transporter (*DAT*), which mediates clearance of dopamine from the synaptic cleft (Kume et al., 2005) and regulates dopamine signaling independent of any specific receptor. The profile of odor-evoked pre-synaptic Ca^{2+} in *DAT* mutants was significantly altered, resembling the phenotype of the *DopR1*/*DopR2* mutant (Figure S5E). These manipulations of dopamine detection and handling confirm that dopaminergic signaling, and not simply DAN activity, contributes to the precise spatial topography of presynaptic Ca^{2+} along KC axons, providing a functional link between molecular and neural mechanisms.

Dopaminergic Modulation of KC-MBON Neurotransmission

Together, our experiments indicate that dopaminergic modulation can acutely modify synaptic responses in discrete subcellular domains along individual KC axons. If this presynaptic modulation resulted in altered neurotransmission to the MBONs, our data would suggest that the state of the DAN network could dynamically regulate the flow of olfactory information to each output pathway. We therefore assessed how DAN activity modifies KC-MBON signaling using electrophysiology to monitor neurotransmission at the resolution of individual synaptic events.

We targeted the γ4 MBON for voltage-clamp recordings as it innervates the compartment exhibiting the most robust dopamine-dependent modulation of KC presynaptic Ca^{2+} (Figure 5B). Recordings were performed in a brain explant where reduced basal activity allowed for the measurement of well-isolated synaptic currents and provided precise control over the neuromodulatory state of synapses. We stimulated KC dendrites in the calyx to evoke excitatory postsynaptic currents (EPSCs) in the γ4 MBON and observed that the strength of these synaptic inputs markedly increased following 58E02+ DAN activation (Figure 6A). Spontaneous synaptic events also were potentiated whether DANs were activated using $P2X_2$ or a red-shifted channelrhodopsin (Figure S6A). The average latency of EPSCs after KC stimulation was 3.8 ± 0.1 ms, consistent with monosynaptic transmission (Kazama and Wilson, 2008), identifying KC-MBON synapses as the site of dopaminergic modulation. Focal application of the inhibitory neurotransmitter GABA onto KC dendrites resulted in the loss of synaptic events, further substantiating KCs as the source of this potentiated synaptic input (Figure S6A). In contrast to the prominent modulation of synaptic currents, activation of 58E02+ DANs had no apparent effect on the baseline membrane voltage or evoked spiking of γ KCs (Figure S6B). Dopaminergic modulation, therefore, potentiates neurotransmission at KC-MBON synapses without appearing to change the intrinsic

excitability of KCs, providing a mechanism to alter the propagation of olfactory signals to each MBON without modifying the underlying KC odor representation.

Compartmental Specificity of Dopaminergic Modulation

Dopamine can act diffusely, regulating circuit properties at a distance from its site of release (Rice et al., 2011). We therefore asked whether DANs modulate synaptic signaling only in the compartments they innervate or more broadly along the lobe. Functional imaging revealed that the response of the γ4 MBON to direct KC stimulation was enhanced after 58E02+ DAN activation (Figures 6B and S6C), consistent with the potentiation measured by electrophysiology. In contrast, activation of the γ4 DAN had no effect on the response of the γ2 MBON (Figure 6D). Likewise, activation of the γ2 DAN strengthened the γ2 MBON response to KC stimulation (Figures 6C and S6C), but resulted in a small but significant depression of activity in the γ4 MBON (Figure 6E). Together, these experiments indicate that the segregated axonal innervation by DANs permits spatially restricted potentiation of KC-MBON neurotransmission, localized to the synapses within a compartment.

State-Dependent Changes in MBON Activity Patterns

Heterogeneous neurotransmission from the synapses along a single axon has been described in the cortex and hippocampus as a possible substrate for independent plasticity between a neuron and its myriad of postsynaptic targets (Markram et al., 1998; Pelkey and McBain, 2007). However, rarely has it been possible to trace the propagation of neural signals from nearby synapses on the same axons to distinct postsynaptic pathways. We took advantage of the compartmentalized architecture of the mushroom body to examine whether the localized synaptic modulation along KC axons results in differential olfactory responses across the MBONs that tile the lobe. We expressed GCaMP6s in pairs of γ MBONs (γ2/γ4 or γ3/γ5, Figure 7A), and we simultaneously measured dendritic Ca^{2+} responses to odor stimuli in their segregated projections. Every odor evoked significantly more robust responses in the γ2 and γ3 MBONs compared to the γ4 and γ5 MBONs (Figure 7B), paralleling the compartmental differences exhibited by KCs to olfactory stimuli (Figure 4C). In contrast, direct stimulation of KCs in a brain explant elicited comparable responses across MBONs (Figure 7C), confirming that, in the absence of in vivo modulation, KCs have the inherent capacity to transmit equivalent signals to the different output pathways of the lobe (Figures 4D, S4D, and S4E).

Together, these observations indicate the odor responses of MBONs are differentially tuned by the activity of their cognate DANs, allowing contextual cues to shape olfactory signaling through the parallel outputs of the lobe. In support of this conclusion, we found that exogenous activation of the γ4 DANs via $P2X_2$ resulted in robust potentiation of the γ4 MBON responses to all odors tested (Figures 7D, S7A, and S7B), while olfactory responses in the γ2 MBON were unaffected (Figure 7E). Similarly, sugar feeding, an appetitive stimulus that activates the γ4/γ5 DANs and inhibits the γ2/γ3 DANs (Figure 2B), enhanced the γ4 MBON odor response relative to the γ2 MBON response (Figure 7F). Thus, acute changes to the state or context of an animal can rapidly gate the transmission of olfactory signals to the MBONs of the lobe, permitting the same odor stimulus to drive distinct patterns of output activity in different contexts.

DAN Activity Bidirectionally Modulates KC-MBON Signaling

Dopamine can modulate synaptic communication in diverse ways—including potentiation or depression of neurotransmission and modifications to both short- and long-term plasticity (Tritsch and Sabatini, 2012). Our data indicate that DAN activation by salient reinforcement experiences can modify the state of KC synapses with enduring consequences to how all subsequent odor signals are processed. In contrast, during associative learning, the contingent pairing of olfactory and dopaminergic reinforcement pathways is thought to alter neurotransmission from odor-specific KC ensembles to allow formation of select olfactory memories (Heisenberg, 2003; Keene and Waddell, 2007). We therefore asked whether coincident activation of KCs and DANs elicits a distinct form of synaptic modulation in comparison to when DANs are activated independently. Remarkably, temporally pairing 58E02+ DAN activation with KC stimulation resulted in depression of KC-evoked γ4 MBON responses, in contrast to the robust potentiation induced by activation of DANs alone (Figures 7G–7I). Interleaving temporally paired and unpaired stimulation protocols produced depression and potentiation within the same preparation, indicating that KC-MBON synapses are capable of rapid and reversible bidirectional plasticity (Figures 7H, S7C, and S7I). Depression of KC-MBON signaling was restricted to the compartment innervated by the activated DANs, suggesting a similar spatial specificity for these opposing forms of dopaminergic modulation (Figure S7J).

If depression of KC-MBON signaling were limited to only KCs co-activated during an olfactory experience, our observations would provide a mechanistic basis for the odor-specific modulation thought to underlie learned olfactory associations within the mushroom body. We therefore monitored the responses of the γ4 MBON to two different odors and then paired the presentation of one odor with 58E02+ DAN stimulation. Following DAN activation, the MBON's response to the paired odor was significantly reduced relative to the unpaired odor (Figure 7J). Thus, DAN activity can bidirectionally modulate KC-MBON signaling, allowing for both odor-independent synaptic potentiation as well as odor-specific depression.

DISCUSSION

In this study, we took advantage of the mushroom body's orderly architecture to gain insight into the circuit mechanisms through which neuromodulation mediates flexible sensory processing. Compartmentalized dopaminergic signaling permits independent tuning of synaptic transmission between an individual KC and its repertoire of postsynaptic MBON targets. As a consequence, the same KC odor representation can evoke different patterns of output activity, depending on the state of the animal and the dopaminergic network. Recent data indicate that the ensemble of MBONs acts in concert to bias an animal's behavioral response to an odor such that altering the balance of their activity can modify the olfactory preferences of both naive and trained animals (Aso et al., 2014a; Lewis et al., 2015; Owald et al., 2015). In accord with such a model, we reveal how a distributed neuromodulatory network is poised to orchestrate plasticity across all 15 compartments of the mushroom body and reweight the net output of the MBONs, allowing for adaptive behavioral responses based on the immediate needs or past experience of the animal.

A Dynamic Neuromodulatory Network

Distinct subsets of DANs are sufficient to drive learned olfactory associations (Aso et al., 2012; Claridge-Chang et al., 2009; Liu et al., 2012; Waddell, 2013; Yamagata et al., 2015), leading to the suggestion they may act autonomously to encode the rewarding or punishing contextual stimuli that assign meaning to an odor. Our data, however, suggest a more complex circuit architecture, in which rich functional interconnectivity between compartments contributes to coordinated and bidirectional patterns of activity across the DAN population. This raises the possibility that reinforcement experiences may be represented by combinatorial patterns of DAN excitation and inhibition in different compartments, endowing the dopaminergic population with a greater capacity to instruct behavior via the limited repertoire of mushroom body outputs. Intriguingly, midbrain dopaminergic neurons responsive to punishment and reward also project to distinct targets in the mammalian brain and display a similar functional opponency as a consequence of reciprocal network interactions (Cohen et al., 2012; Lammel et al., 2012, 2014; Lerner et al., 2015). Thus, the concerted and partially antagonistic action of neuromodulatory pathways may represent a general and conserved circuit principle for generating adaptive behavioral responses.

Distinct DAN network activity states are evoked by electric shock and sugar ingestion, reinforcers classically used in associative olfactory conditioning paradigms because of their strong inherent valence. However, similarly distributed patterns of DAN activity are correlated with the fly's motor activity, implying that an animal's behavioral state might serve as a reinforcement stimulus that itself drives synaptic plasticity to shape odor processing. Metabolic states, such as thirst and hunger, have been shown to gate appetitive reinforcement by water and sugar rewards (Burke et al., 2012; Huetteroth et al., 2015; Lin et al., 2014), permitting state-dependent formation of olfactory associations only in motivated animals. Our data highlight an additional facet of how an animal's internal state can regulate dopamine release to adjust the salience of contextual cues. Together, these observations indicate that the distributed DAN network integrates information about external context and internal state with MBON feedback to represent the moment-by-moment experience of an animal and dynamically regulate the flow of olfactory signals through the mushroom body.

Spatially Precise Synaptic Modulation

The independent regulation of synapses along an axon is thought to permit a single neuron to convey specialized information to different downstream targets, providing additional flexibility and computational power to neural circuits (Markram et al., 1998; Pelkey and McBain, 2007). In the mushroom body, synapse-specific plasticity is achieved through spatially restricted patterns of dopaminergic modulation that divide a KC axon into functionally distinct segments. Thus, the ensemble of synapses within a compartment, as the site of convergence for sensory and contextual signals, represents the elementary functional unit that underlies experience-dependent mushroom body output.

Within a compartment, multiple neuromodulatory mechanisms appear to shape synaptic signaling. We observed broad potentiation of KC-MBON synapses after DAN activation but odor-specific depression if DANs were coincidently activated with KCs, consistent with the

synaptic changes previously proposed to occur after learning (Aso et al., 2014b; Owald et al., 2015; Séjourné et al., 2011). Taken together, these findings indicate that neuromodulation in the mushroom body instructs opposing forms of synaptic plasticity, analogous to the bidirectional tuning of synaptic strength by dopamine in mammalian brain centers (Huang et al., 2004; Shen et al., 2008; Tritsch and Sabatini, 2012). The molecular mechanisms through which dopamine can direct diverse synaptic changes within a compartment remain to be elucidated, but they may depend on signaling through different dopamine receptors or downstream signaling cascades that function as coincidence detectors. Indeed, while *DopR1* in KCs is essential to the formation of learned olfactory associations (Kim et al., 2007; Qin et al., 2012), we find this receptor plays only a subtle role in the context-dependent patterning of Ca^{2+} along their axons. Conversely, *DopR2* strongly influences the topography of presynaptic Ca^{2+} along KC axons, in accord with evidence that tonic release of dopamine during ongoing behavior acts through this receptor to interfere with the maintenance of specific learned olfactory associations (Berry et al., 2012, 2015). Thus, distinct molecular pathways may transform the same dopaminergic reinforcement signals into synaptic changes of opposite polarity to shape olfactory processing based on both the present context and prior experiences of an individual.

A Common Integrative Circuit Architecture for Adaptive Responses

The mushroom body has been most extensively studied as a site for associative learning (Heisenberg, 2003; Keene and Waddell, 2007) in which the temporal pairing of an odor with a reinforcement experience selectively alters subsequent behavioral responses to that odor. Our data suggest that the convergence of DAN network activity and KC olfactory representations within the mushroom body lobes may drive associative plasticity in each compartment, allowing the odor tuning of the MBON repertoire to reflect the unique experiences of an individual (Hige et al., 2015). However, our observations also provide insight into the mushroom body's broader role in the context-dependent regulation of innate behaviors (Lewis et al., 2015; Owald et al., 2015). The ongoing activity of the distributed DAN network, encoding information about an animal's current environmental context and behavioral state, is poised to continuously reconfigure the activity patterns of the MBON population to allow for adaptive responses based on the acute needs of the animal. This context-dependent synaptic modulation could potentially erode odor-specific learned associations within the mushroom body, permitting the immediate circumstances of an animal to dominate over previously learned olfactory associations that may no longer be predictive or relevant. The axons of MBONs ultimately converge with output pathways from the lateral horn (Aso et al., 2014a, 2014b), a *Drosophila* brain center thought to mediate stereotyped responses to odors, providing a potential substrate for learned and context-dependent output from the mushroom body to influence inherent olfactory preferences.

Thus, the dual role of neuromodulation in the mushroom body—to select among alternative circuit states that regulate both innate and learned behaviors—is reminiscent of its function in other higher integrative brain centers. In the basal ganglia, for example, different temporal patterns of dopamine release are thought to select the relevant circuit configurations that control inherently motivated behaviors as well as reinforcement learning (Graybiel et al., 1994; Grillner et al., 2005; Kreitzer and Malenka, 2008; Yin and Knowlton, 2006). The

generation of flexible behavioral responses based on experience, whether past or present, may therefore rely on common integrative brain structures in which neuromodulatory networks act with exquisite spatial precision to shape sensory processing.

EXPERIMENTAL PROCEDURES

Detailed methods associated with all procedures below are available in the Supplemental Experimental Procedures.

Fly Stocks

A detailed list of fly genotypes can be found in the Supplemental Experimental Procedures. The sytGCaMP was generated by linking the GCaMP6s and *Drosophila* synaptotagmin 1 coding sequences through a 3×GS linker. The resulting construct (sytGCaMP) was used to generate transgenic flies by PhiC31-based integration into attp40, attp5, and VK00005 (BestGene).

Functional Imaging

All functional imaging experiments were performed on an Ultima two-photon laser-scanning microscope (Bruker Nanosystems) as previously described (Ruta et al., 2010). For volumetric imaging, the laser was directed through an 8-kHz resonant scanning galvonometer and the objective was controlled by a piezo-electric Z-focus. Z planes (12–18 planes), spaced ~2 μm apart, were defined to encompass the entire volume of the γ lobe and imaged at ~1.5 Hz. Odor stimulation was achieved by directing a continuous stream (400–500 ml/min) of air through a 2-mm-diameter teflon tube at the fly. At a trigger, 5%–10% of the total airstream was diverted from a 10-ml glass vial containing paraffin oil to to a vial containing odorants diluted in paraffin oil.

Electrophysiology

The γ4 MBON and KC soma were targeted for patch recording using GCaMP or GFP fluorescence. Recordings were carried out as previously described (Ruta et al., 2010). The membrane potential during voltage clamp was nominally −70 mV. At this voltage, unclamped action potentials rarely broke through and were readily detected by their large amplitude.

Exogenous Activation of KCs and DANs

Glass stimulating electrodes (resistance of 7–10 MΩ) were filled with 2 mM ATP or 10 mM acetylcholine. To stimulate DANs and MBONs expressing the $P2X_2$ receptor, electrodes were positioned dorsal to the mushroom body's medial lobes at the site of DAN dendritic and MBON axonal innervation and ATP was applied by a positive pressure pulse. KCs were stimulated by iontophoresing acetylcholine into the calyx using voltage pulses. For paired trials, KC and DAN stimulation were carried out within <500 ms of each other. For unpaired trials, KC and DAN stimulation were separated by >45 s. All DAN activation experiments were unpaired unless noted.

Tethered Fly Behavior

A Point Grey Firefly Camera with Infinity Lens (94-mm focal length) was focused on a fly illuminated by infrared light-emitting diodes (LEDs). Video was captured at 30 frames/s. Fly motion traces were extracted using a custom MATLAB script. For sugar feeding, flies were fasted for 20–26 hr and then offered a paper wick soaked in 0.2–1 M sucrose using a motorized micromanipulator (Scientifica). For punitive shock, steel electrode leads were positioned on a fly's abdomen and 0.5-s pulses of 60–150 V were applied from a stimulator (Grass Technologies).

Supplementary Material

Refer to Web version on PubMed Central for supplementary material.

ACKNOWLEDGMENTS

We thank Leslie Vosshall, Cori Bargmann, Richard Axel, Larry Abbott, Sandeep Datta, Barbara Noro, Daisuke Hattori, Meg Younger, and members of the V.R. lab for valuable discussion. We thank Donovan Ventimiglia, Tim Ryan, Ari Zolin, Eliezer Pickholtz, and Josh Salvi for technical advice. R.C. was supported by a David Rockefeller Graduate Student Fellowship. V.R. is a New York Stem Cell Foundation Robertson Neuroscience Investigator and was supported by a Pew Biomedical Scholar Award, a McKnight Scholar Award, the Alfred P. Sloan Foundation, an Irma T. Hirschl Award, a Sinsheimer Foundation Award, and an NIH New Innovator Award (DP2 NS0879422013).

REFERENCES

Aso Y, Herb A, Ogueta M, Siwanowicz I, Templier T, Friedrich AB, Ito K, Scholz H, Tanimoto H. Three dopamine pathways induce aversive odor memories with different stability. PLoS Genet. 2012; 8:e1002768. [PubMed: 22807684]

Aso Y, Hattori D, Yu Y, Johnston RM, Iyer NA, Ngo T-TB, Dionne H, Abbott LF, Axel R, Tanimoto H, Rubin GM. The neuronal architecture of the mushroom body provides a logic for associative learning. eLife. 2014a; 3:e04577. [PubMed: 25535793]

Aso Y, Sitaraman D, Ichinose T, Kaun KR, Vogt K, Belliart-Guérin G, Plaçais P-Y, Robie AA, Yamagata N, Schnaitmann C, et al. Mushroom body output neurons encode valence and guide memory-based action selection in Drosophila. eLife. 2014b; 3:e04580. [PubMed: 25535794]

Bargmann CI. Beyond the connectome: how neuromodulators shape neural circuits. BioEssays. 2012; 34:458–465. [PubMed: 22396302]

Beier KT, Steinberg EE, DeLoach KE, Xie S, Miyamichi K, Schwarz L, Gao XJ, Kremer EJ, Malenka RC, Luo L. Circuit architecture of VTA dopamine neurons revealed by systematic input-output mapping. Cell. 2015; 162:622–634. [PubMed: 26232228]

Beninger RJJ. The role of dopamine in locomotor activity and learning. Brain Res. 1983; 287:173–196. [PubMed: 6357357]

Berry JA, Cervantes-Sandoval I, Nicholas EP, Davis RL. Dopamine is required for learning and forgetting in Drosophila. Neuron. 2012; 74:530–542. [PubMed: 22578504]

Berry JA, Cervantes-Sandoval I, Chakraborty M, Davis RL. Sleep facilitates memory by blocking dopamine neuron-mediated forgetting. Cell. 2015; 161:1656–1667. [PubMed: 26073942]

Bromberg-Martin ES, Matsumoto M, Hikosaka O. Dopamine in motivational control: rewarding, aversive, and alerting. Neuron. 2010; 68:815–834. [PubMed: 21144997]

Burke CJ, Huetteroth W, Owald D, Perisse E, Krashes MJ, Das G, Gohl D, Silies M, Certel S, Waddell S. Layered reward signalling through octopamine and dopamine in Drosophila. Nature. 2012; 492:433–437. [PubMed: 23103875]

Campbell RA, Honegger KS, Qin H, Li W, Demir E, Turner GC. Imaging a population code for odor identity in the Drosophila mushroom body. J. Neurosci. 2013; 33:10568–10581. [PubMed: 23785169]

Caron SJC, Ruta V, Abbott LF, Axel R. Random convergence of olfactory inputs in the Drosophila mushroom body. Nature. 2013; 497:113–117. [PubMed: 23615618]

Claridge-Chang A, Roorda RD, Vrontou E, Sjulson L, Li H, Hirsh J, Miesenböck G. Writing memories with light-addressable reinforcement circuitry. Cell. 2009; 139:405–415. [PubMed: 19837039]

Cohen JY, Haesler S, Vong L, Lowell BB, Uchida N. Neurontype-specific signals for reward and punishment in the ventral tegmental area. Nature. 2012; 482:85–88. [PubMed: 22258508]

Fiorillo CD, Song MR, Yun SR. Multiphasic temporal dynamics in responses of midbrain dopamine neurons to appetitive and aversive stimuli. J. Neurosci. 2013; 33:4710–4725. [PubMed: 23486944]

Graybiel AM, Aosaki T, Flaherty AW, Kimura M. The basal ganglia and adaptive motor control. Science. 1994; 265:1826–1831. [PubMed: 8091209]

Grillner S, Hellgren J, Ménard A, Saitoh K, Wikström MA. Mechanisms for selection of basic motor programs–roles for the striatum and pallidum. Trends Neurosci. 2005; 28:364–370. [PubMed: 15935487]

Gruntman E, Turner GC. Integration of the olfactory code across dendritic claws of single mushroom body neurons. Nat. Neurosci. 2013; 16:1821–1829. [PubMed: 24141312]

Heisenberg M. Mushroom body memoir: from maps to models. Nat. Rev. Neurosci. 2003; 4:266–275. [PubMed: 12671643]

Hige T, Aso Y, Rubin GM, Turner GC. Plasticity-driven individualization of olfactory coding in mushroom body output neurons. Nature. 2015; 526:258–262. [PubMed: 26416731]

Huang Y-Y, Simpson E, Kellendonk C, Kandel ER. Genetic evidence for the bidirectional modulation of synaptic plasticity in the prefrontal cortex by D1 receptors. Proc. Natl. Acad. Sci. USA. 2004; 101:3236–3241. [PubMed: 14981263]

Huetteroth W, Perisse E, Lin S, Klappenbach M, Burke C, Waddell S. Sweet taste and nutrient value subdivide rewarding dopaminergic neurons in Drosophila. Curr. Biol. 2015; 25:751–758. [PubMed: 25728694]

Kazama H, Wilson RI. Homeostatic matching and nonlinear amplification at identified central synapses. Neuron. 2008; 58:401–413. [PubMed: 18466750]

Keene AC, Waddell S. Drosophila olfactory memory: single genes to complex neural circuits. Nat. Rev. Neurosci. 2007; 8:341–354. [PubMed: 17453015]

Kim Y-C, Lee H-G, Han K-A. D1 dopamine receptor dDA1 is required in the mushroom body neurons for aversive and appetitive learning in Drosophila. J. Neurosci. 2007; 27:7640–7647. [PubMed: 17634358]

Kreitzer AC, Malenka RC. Striatal plasticity and basal ganglia circuit function. Neuron. 2008; 60:543–554. [PubMed: 19038213]

Kume K, Kume S, Park SK, Hirsh J, Jackson FR. Dopamine is a regulator of arousal in the fruit fly. J. Neurosci. 2005; 25:7377–7384. [PubMed: 16093388]

Lammel S, Lim BK, Ran C, Huang KW, Betley MJ, Tye KM, Deisseroth K, Malenka RC. Input-specific control of reward and aversion in the ventral tegmental area. Nature. 2012; 491:212–217. [PubMed: 23064228]

Lammel S, Lim BK, Malenka RC. Reward and aversion in a heterogeneous midbrain dopamine system. Neuropharmacology. 2014; 76(Pt B):351–359. [PubMed: 23578393]

Lerner TN, Shilyansky C, Davidson TJ, Evans KE, Beier KT, Zalocusky KA, Crow AK, Malenka RC, Luo L, Tomer R, Deisseroth K. Intact-brain analyses reveal distinct information carried by SNc dopamine subcircuits. Cell. 2015; 162:635–647. [PubMed: 26232229]

Lewis LPC, Siju KP, Aso Y, Friedrich AB, Bulteel AJB, Rubin GM, Grunwald Kadow IC. A Higher Brain Circuit for Immediate Integration of Conflicting Sensory Information in Drosophila. Curr. Biol. 2015; 25:2203–2214. [PubMed: 26299514]

Lin S, Owald D, Chandra V, Talbot C, Huetteroth W, Waddell S. Neural correlates of water reward in thirsty Drosophila. Nat. Neurosci. 2014; 17:1536–1542. [PubMed: 25262493]

Liu C, Plaçais P-Y, Yamagata N, Pfeiffer BD, Aso Y, Friedrich AB, Siwanowicz I, Rubin GM, Preat T, Tanimoto H. A subset of dopamine neurons signals reward for odour memory in Drosophila. Nature. 2012; 488:512–516. [PubMed: 22810589]

Mao Z, Davis RL. Eight different types of dopaminergic neurons innervate the Drosophila mushroom body neuropil: anatomical and physiological heterogeneity. Front. Neural Circuits. 2009; 3:5. [PubMed: 19597562]

Marder E. Neuromodulation of neuronal circuits: back to the future. Neuron. 2012; 76:1–11. [PubMed: 23040802]

Markram H, Wang Y, Tsodyks M. Differential signaling via the same axon of neocortical pyramidal neurons. Proc. Natl. Acad. Sci. USA. 1998; 95:5323–5328. [PubMed: 9560274]

Owald D, Felsenberg J, Talbot CB, Das G, Perisse E, Huetteroth W, Waddell S. Activity of defined mushroom body output neurons underlies learned olfactory behavior in Drosophila. Neuron. 2015; 86:417–427. [PubMed: 25864636]

Pelkey KA, McBain CJ. Differential regulation at functionally divergent release sites along a common axon. Curr. Opin. Neurobiol. 2007; 17:366–373. [PubMed: 17493799]

Qin H, Cressy M, Li W, Coravos JS, Izzi SA, Dubnau J. Gamma neurons mediate dopaminergic input during aversive olfactory memory formation in Drosophila. Curr. Biol. 2012; 22:608–614. [PubMed: 22425153]

Redgrave P, Gurney K. The short-latency dopamine signal: a role in discovering novel actions? Nat. Rev. Neurosci. 2006; 7:967–975. [PubMed: 17115078]

Regehr WG. Short-term presynaptic plasticity. Cold Spring Harb. Perspect. Biol. 2012; 4:a005702. [PubMed: 22751149]

Rice ME, Patel JC, Cragg SJ. Dopamine release in the basal ganglia. Neuroscience. 2011; 198:112–137. [PubMed: 21939738]

Ruta V, Datta SR, Vasconcelos ML, Freeland J, Looger LL, Axel R. A dimorphic pheromone circuit in Drosophila from sensory input to descending output. Nature. 2010; 468:686–690. [PubMed: 21124455]

Schultz W, Dayan P, Montague PR. A neural substrate of prediction and reward. Science. 1997; 275:1593–1599. [PubMed: 9054347]

Séjourné J, Plaçais P-Y, Aso Y, Siwanowicz I, Trannoy S, Thoma V, Tedjakumala SR, Rubin GM, Tchénio P, Ito K, et al. Mushroom body efferent neurons responsible for aversive olfactory memory retrieval in Drosophila. Nat. Neurosci. 2011; 14:903–910. [PubMed: 21685917]

Shen W, Flajolet M, Greengard P, Surmeier DJ. Dichotomous dopaminergic control of striatal synaptic plasticity. Science. 2008; 321:848–851. [PubMed: 18687967]

Tanaka NK, Tanimoto H, Ito K. Neuronal assemblies of the Drosophila mushroom body. J. Comp. Neurol. 2008; 508:711–755. [PubMed: 18395827]

Tritsch NX, Sabatini BL. Dopaminergic modulation of synaptic transmission in cortex and striatum. Neuron. 2012; 76:33–50. [PubMed: 23040805]

Waddell S. Reinforcement signalling in Drosophila; dopamine does it all after all. Curr. Opin. Neurobiol. 2013; 23:324–329. [PubMed: 23391527]

Wise RA. Dopamine, learning and motivation. Nat. Rev. Neurosci. 2004; 5:483–494. [PubMed: 15152198]

Yamagata N, Ichinose T, Aso Y, Plaçais P-Y, Friedrich AB, Sima RJ, Preat T, Rubin GM, Tanimoto H. Distinct dopamine neurons mediate reward signals for short- and long-term memories. Proc. Natl. Acad. Sci. USA. 2015; 112:578–583. [PubMed: 25548178]

Yin HH, Knowlton BJ. The role of the basal ganglia in habit formation. Nat. Rev. Neurosci. 2006; 7:464–476. [PubMed: 16715055]

Highlights

- Mushroom body dopaminergic neurons act in concert to represent contextual cues
- Dopamine bidirectionally modifies synapses in precise domains along Kenyon cell axons
- Odor signals are differentially conveyed to each postsynaptic target of a Kenyon cell
- Activity of output pathways depends on animal's external context or internal state

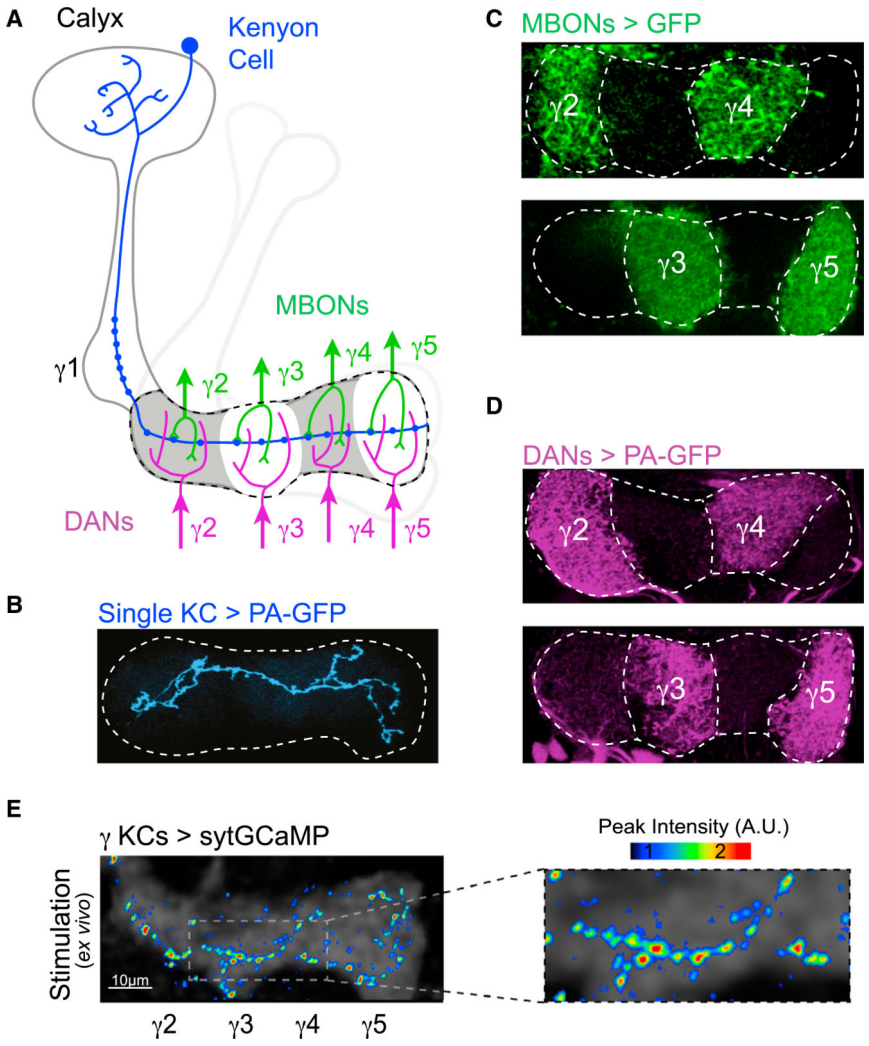

Figure 1. Compartmentalized Architecture of the Mushroom Body

(A) Schematic of mushroom body anatomy focusing on the γ lobe. Each γ Kenyon cell (KC, blue) receives olfactory input in the calyx and projects a single axon into the γ lobe (dashed line). KCs form en passant synapses with mushroom body output neurons (MBONs, green) and receive modulatory input from dopaminergic neurons (DANs, magenta) within discrete anatomic compartments (shown for γ2–γ5).

(B) A single γ KC axon photolabeled with PA-GFP projects its axon across the complete length of the lobe (dashed line).

(C) Segregated dendritic innervation of MBONs is revealed by expression of GFP in pairs of MBONs in each panel using MBON-specific drivers.

(D) Compartmentalized axonal projections of DANs photolabeled with PA-GFP in alternating compartments. PA-GFP is expressed under the TH and DDC promoters.

(E) sytGCaMP expressed in all γ KCs with only a single KC functionally activated. Maximum intensity projection shows peak fluorescence from multiple T-series in different Z planes. Magnified view shows individual KC synaptic puncta (right).

See also Figure S1.

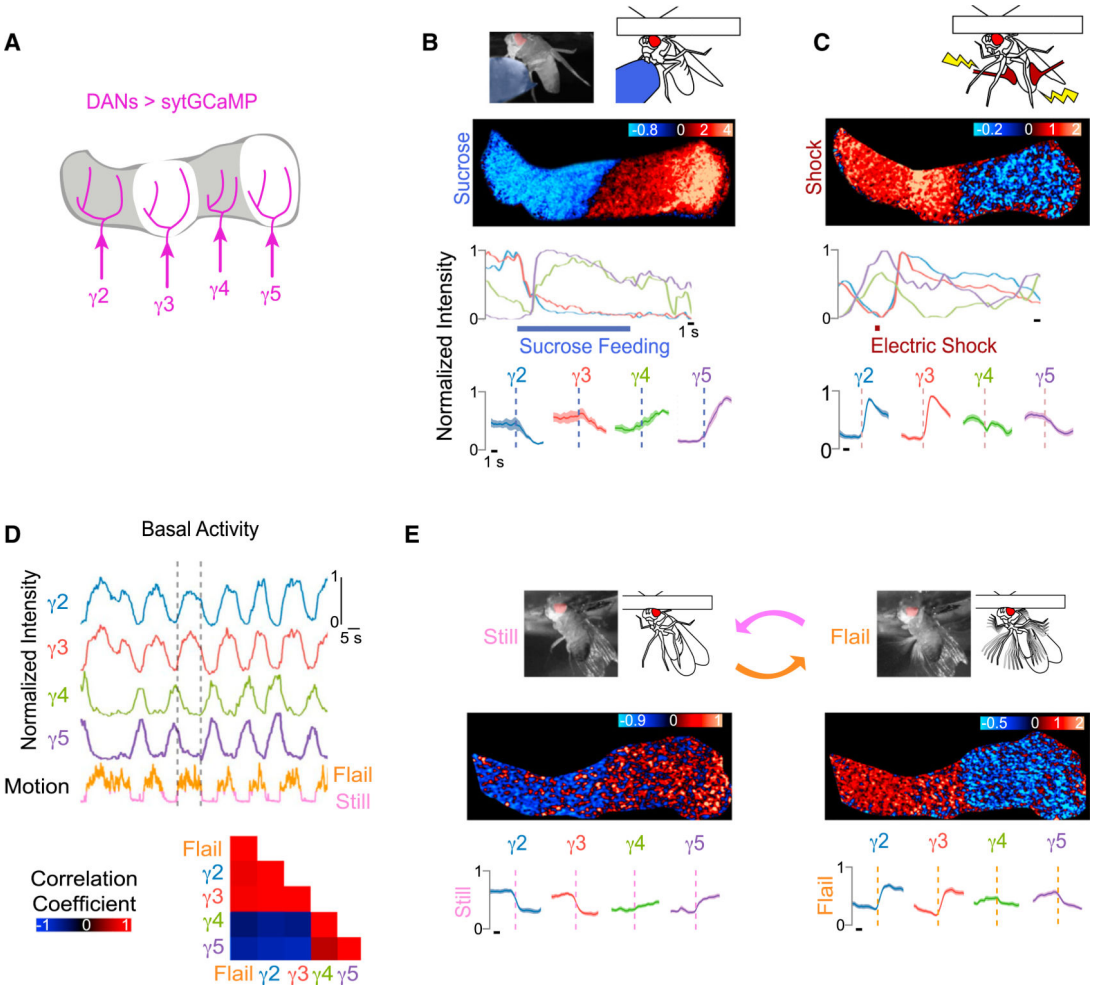

Figure 2. DAN Network Activity Reflects Both External Sensory Stimuli and Internal Behavioral State

(A) The sytGCaMP was expressed in DANs of all γ-lobe compartments, driven by the combination of TH and DDC promoters and imaged in response to sucrose ingestion and electric shock.

(B and C) Sucrose ingestion and electric shock. Schematic of stimulus (top) with representative heatmap ($\Delta F/F_0$) and normalized intensity trace of DAN sytGCaMP response to the stimulus (B, sucrose; C, shock) below are shown. (Bottom) Stimulus-triggered averages ± SEM for DANs of each compartment are shown. (B, n = 10 traces in nine flies; C, n = 21 traces in 11 flies). Fluorescence in other lobes is masked for clarity. Black scale bar indicates 1 s throughout figures unless otherwise noted.

(D) Representative normalized fluorescence traces of γ lobe DANs aligned to fly's motion (top). Dashed lines delineate start and end of a single representative bout of flailing. Cross-correlations between motion trace and activity in DANs of each compartment are shown (bottom, n = 12 traces in six flies).

(E) Schematic and still image from video showing the fly in flailing (right) and quiescent (left) behavioral states (top). Representative heatmap ($\Delta F/F_0$) of DAN activity in response to start and stop of flailing is shown (middle). Average DAN fluorescence ± SEM in each

compartment aligned to the start and stop of flailing is shown (bottom, n = 14 traces in six flies).

See also Figure S2, Table S1, and Movies S1 and S2.

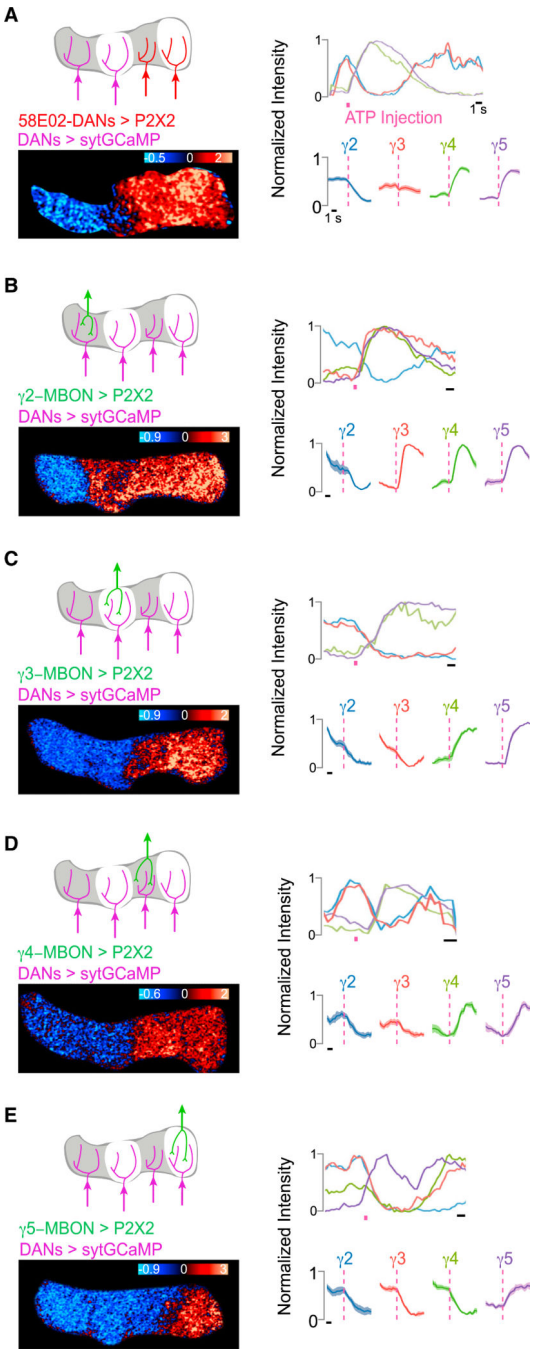

Figure 3. Functional Communication between Compartments Coordinates DAN Network Activity

(A–E) DAN sytGCaMP activity patterns evoked by activation of $P2X_2$ expressed in the (A) 58E02+ DANs innervating γ4-5, (B) γ2 MBON, (C) γ3 MBON, (D) γ4 MBON, and (E) γ5 MBON. The sytGCaMP was expressed in DANs of all γ-lobe compartments using the TH and DDC promoters. Schematic of stimulus (top left), representative heatmap (bottom left, $\Delta F/F_0$), normalized intensity trace for representative experiment shown (top right), and stimulus-triggered averages ± SEM for DANs of each compartment (bottom right) are

shown. ATP stimulation is shown as pink bar (58E02, n = 8; γ2, n = 8; γ3, n = 8; γ4, n = 8; γ5, n = 12).

See also Table S1.

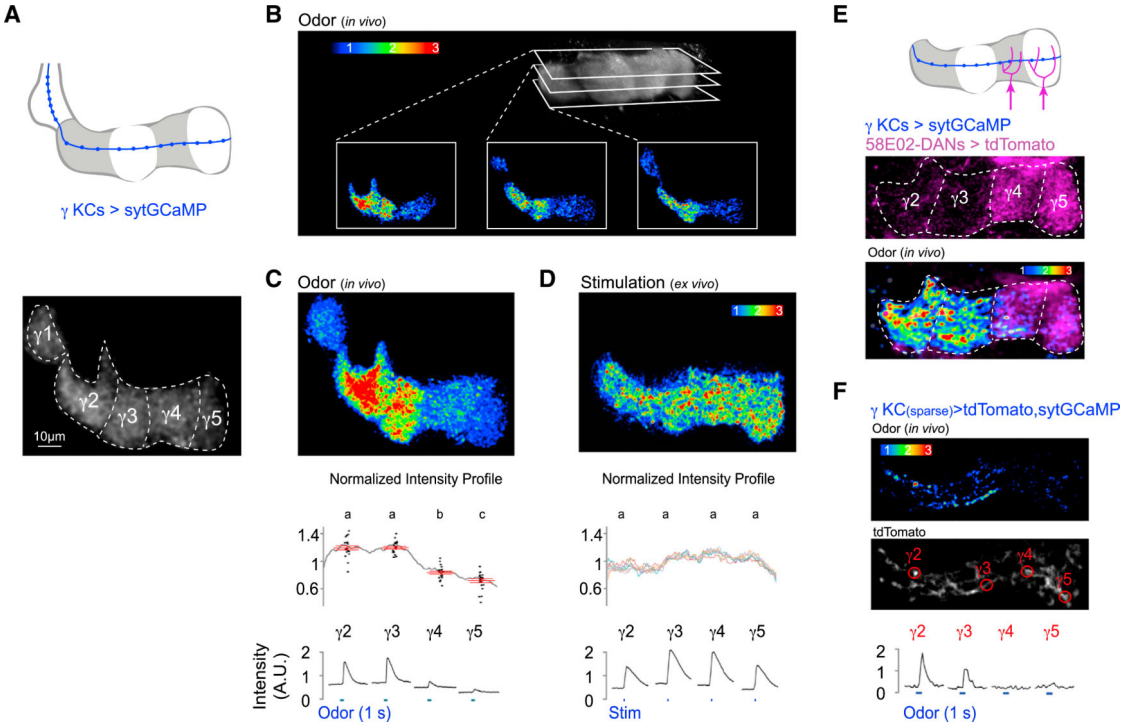

Figure 4. Compartmentalized Ca^{2+} Domains along KC Axons In Vivo

(A) Schematic (top) and representative basal fluorescence of sytGCaMP expressed in γ KCs labeled with approximate compartmental borders (bottom) are shown.

(B) Volumetric two-photon resonant imaging of odor-evoked sytGCaMP reveals asymmetric presynaptic Ca^{2+} in γ KCs in each imaging plane.

(C) Maximum-intensity Z-projection of all 15 imaging planes sampled through the γ lobe in the example shown in (B) (top). Average normalized odor-evoked profile of sytGCaMP fluorescence intensity along the γ lobe (gray line, n = 21 flies) and peak intensity for each compartment (black dots, n = 21) with mean ± SEM in red (middle) are shown. Odor-evoked time courses were imaged in each compartment for representative experiment shown above (bottom, blue lines indicate 1-s odor stimulus).

(D) Representative image of sytGCaMP signal in γ KCs in response to direct stimulation of KCs by acetylcholine iontophoresis into the mushroom body calyx in a brain explant (top). Normalized intensity profiles for ex vivo stimulation across a range of iontophoretic voltages (1–10 V) with average profile for each voltage in a different colored line are shown (n = 6). Stimulation-evoked time courses were imaged in each compartment for representative experiment shown above (bottom, blue lines indicate stimulation).

(E) tdTomato expressed in γ4 and γ5 DANs using 58E02-LexA (top, middle). Compartmentalized KC sytGCaMP responses in the same fly shows synaptic Ca^{2+} domains have sharp boundaries that align to the border between γ3 and γ4 compartments.

(F) Odor response in a sparse subset of γ KCs expressing sytGCaMP (heatmap, top) and tdTomato (grayscale, middle). Odor-evoked time courses were measured at individual synaptic boutons (bottom).

All KC heatmaps in this figure represent peak fluorescence. Values marked with different lowercase letters represent significant differences ($p < 0.05$ by t test with correction for multiple comparisons).

See also Figures S3 and S4 and Movie S3.

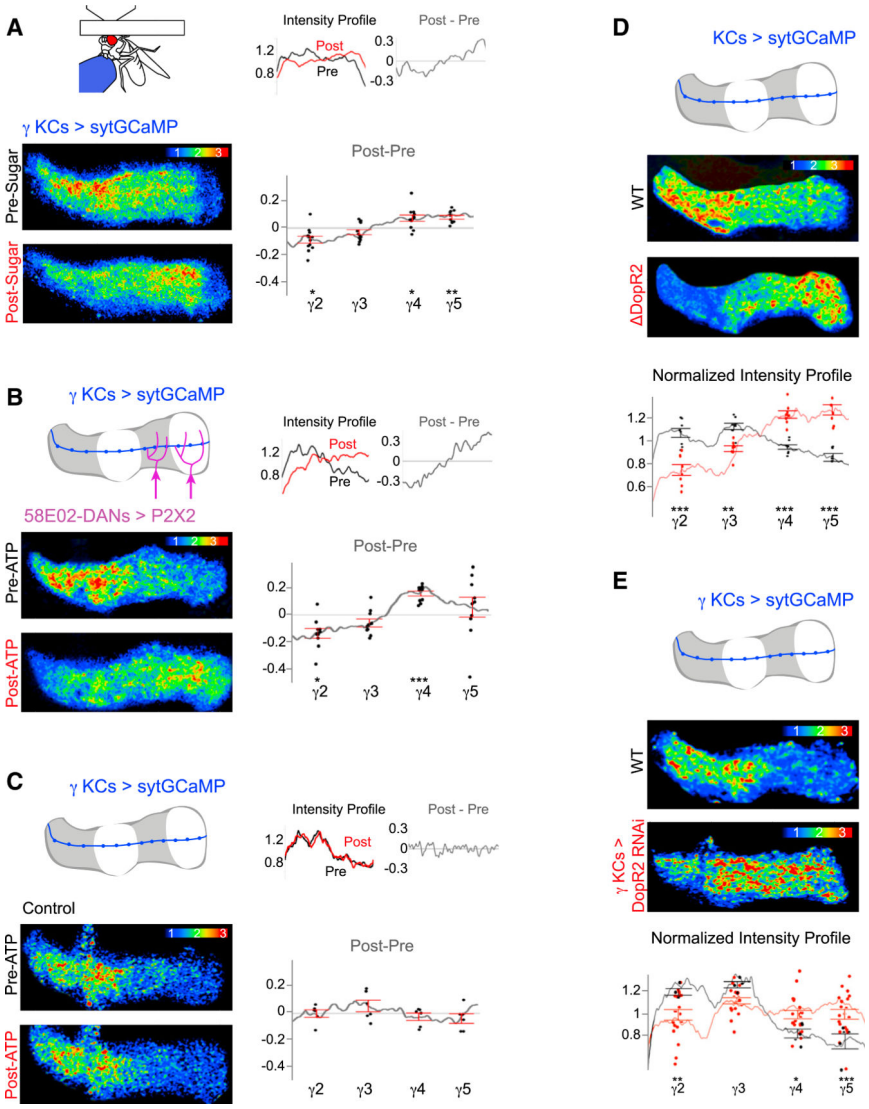

Figure 5. Dopaminergic Signaling Shapes the Distribution of KC Presynaptic Ca^{2+}

(A) Representative odor-evoked KC sytGCaMP response before and after sucrose ingestion (bottom left). Normalized intensity profiles pre- and post-sugar ingestion and the change due to sugar feeding (post-pre) for the representative images are shown (top right). Average change in normalized intensity profile induced by sugar ingestion is shown (bottom right, n = 11 flies).

(B) Schematic of γ lobe $P2X_2$ expression under the 58E02 promoter (top left) and representative odor-evoked responses in γ KCs expressing sytGCaMP, pre- and post-activation of 58E02+ DANs with ATP (bottom left). Normalized intensity profiles and change due to DAN activation for the representative images are shown (top right). Average change in normalized intensity profile induced by DAN activation is shown (bottom right, n = 10 flies).

(C) As in (B), but all are shown in control flies lacking $P2X_2$ expression (n = 6 flies).

(D) Representative odor-evoked response of γ KCs expressing sytGCaMP in DopR2 mutant and wild-type flies (top). Fluorescence in other lobes is masked for clarity. Average

normalized odor-evoked profile across the γ lobe and compartmental averages (bottom) in flies mutant for DopR2 (red, n = 8) and wild-type (black, n = 8) are shown.
(E) As in (D), but this compares γ KC-specific knockdown of DopR2 using RNAi (red, n = 14) to wild-type flies (black, n = 5).
All KC heatmaps in this figure represent peak fluorescence to odor stimulation (Experimental Procedures). Error bars in all panels are SEM. Significant differences in relative compartment intensity compared to wild-type are indicated as follows: *$p < 0.05$, **$p < 0.005$, and ***$p < 0.0005$.
See also Figure S5.

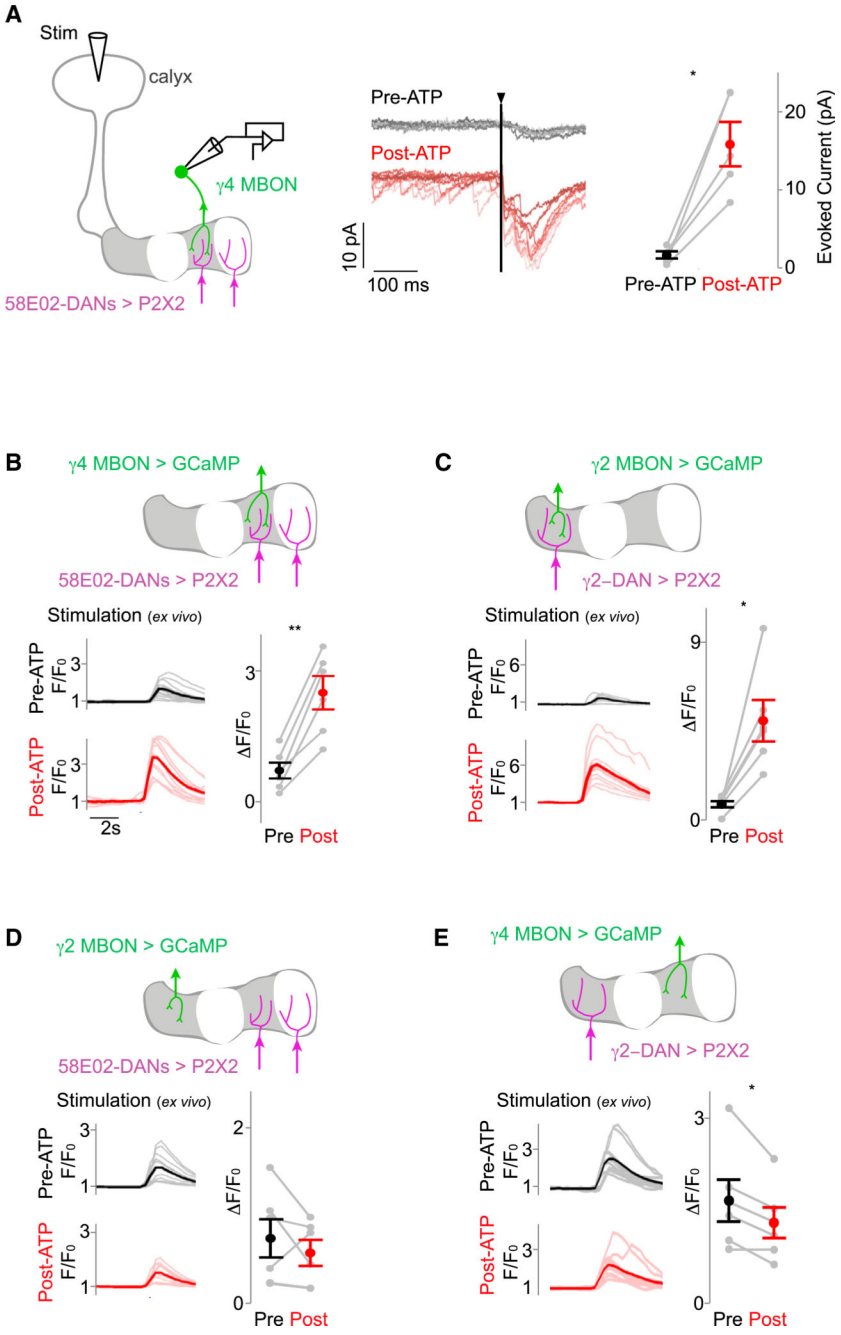

Figure 6. DANs Selectively Potentiate KC-MBON Synaptic Transmission in Individual Compartments

(A) Schematic of experimental setup. Synaptic currents were measured in the γ4 MBON (green) by voltage-clamp recordings in response to direct KC stimulation by acetylcholine iontophoresis in the calyx (Stim). $P2X_2$-expressing 58E02+ DANs (magenta) were activated by local ATP injection (left). Representative γ4 MBON recordings (center) show overlay of ten KC stimulations pre- (grayscale) and post-(redscale) activation of 58E02+ DANs by ATP injection. Note the potentiation evident in both spontaneous and evoked EPSCs. Vertical line denotes 2-ms KC stimulation. Amplitude of evoked currents in the γ4 MBON

pre- and post-ATP injection is shown (right, average of ten stimulations each in n = 5 recordings). (B–E) MBON responses to KC stimulation are potentiated by activation of DANs within the same compartment, but not in other compartments. Schematic (top), time courses (bottom left), and quantification of responses to KC stimulation (bottom right) before and after ATP injection were recorded in (B) the γ4 MBON with activation of the γ4-γ5 (58E02+) DANs (n = 6), (C) the γ2 MBON with activation of the γ2 DAN (n = 6), (D) the γ2 MBON with activation of the γ4-5 DANs (n = 6), and (E) the γ4 MBON with activation of the γ2 DAN (n = 6). All pairwise comparisons plot mean ± SEM. Significance of change after activation is indicated as follows: *$p < 0.05$ and **$p < 0.005$.
See also Figure S6.

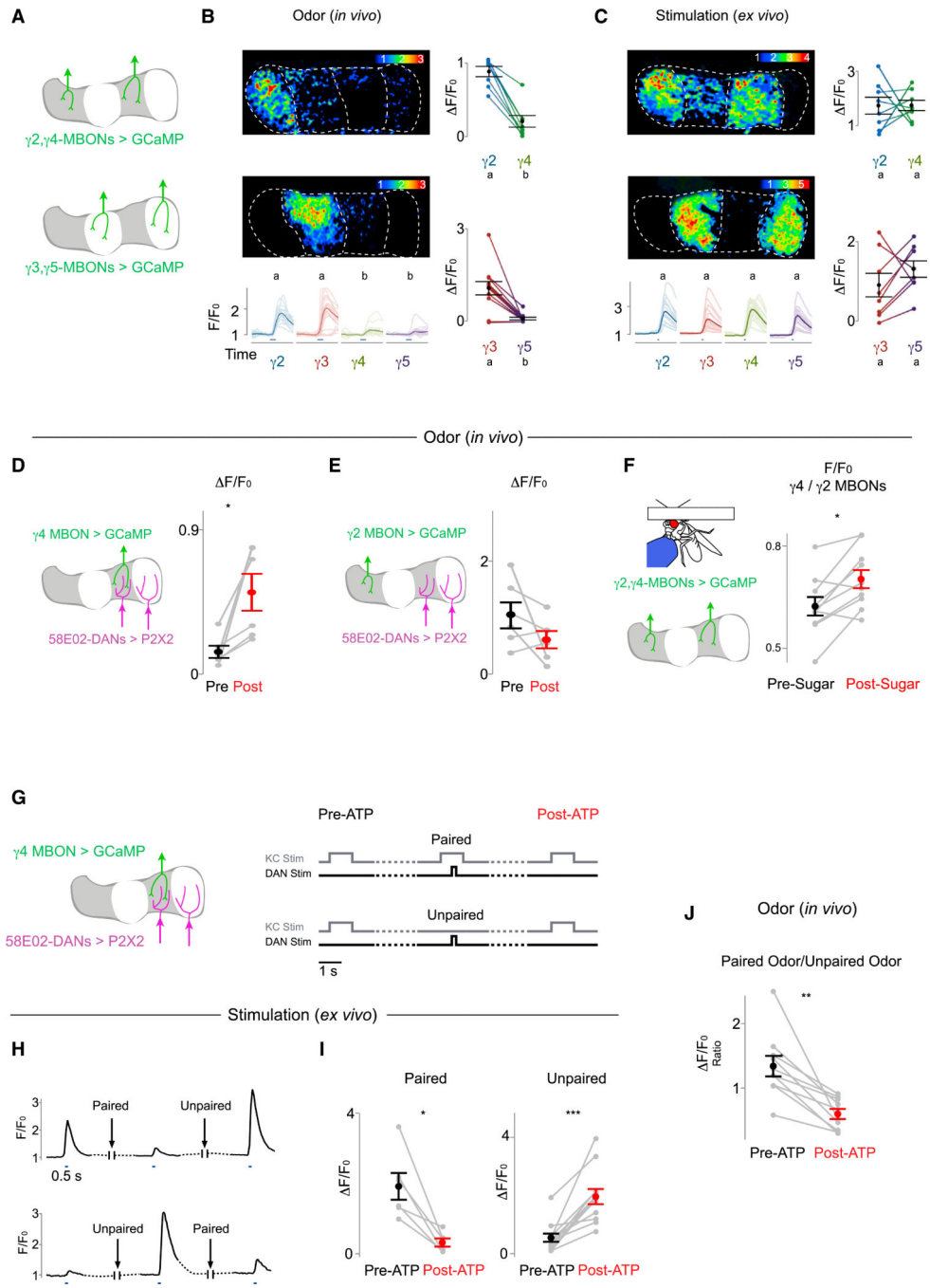

Figure 7. State-Dependent and Bidirectional Modulation of KC-MBON Signaling

(A) Schematic shows pairs of MBONs expressing soluble GCaMP6s used for functional imaging in (B) and (C).

(B and C) Representative heatmaps of evoked fluorescence (top left in each panel, $\Delta F/F_0$), time courses (bottom left), and scatterplots (right) of responses to odor stimuli (blue line) in pairs of MBONs in vivo (B, n = 8 for γ2 versus γ4, n = 11 for γ3 versus γ5) and evoked by calycal stimulation in a brain explant (C, n = 8 for each pair). Values marked with different

lowercase letters represent significant differences ($p < 0.05$ by t test with correction for multiple comparisons).

(D and E) MBON olfactory responses are potentiated by activation of DANs within the same compartment, but not in other compartments. (D) Schematic (left) and quantification of γ4 MBON odor responses before and after stimulation of the γ4-5 (58E02+) DANs are shown (n = 6, right). (E) As in (D), but γ2 MBON response with activation of the γ4-5 DANs was quantified (n = 6).

(F) Ratio between odor-evoked responses in the γ4 MBON and γ2 MBON before and after sugar feeding is shown (n = 10).

(G) Schematic (left) and experimental design (right) for (H)–(J). The γ4 MBON responses to direct KC stimulation (in H–I) or odor stimuli (in J) were recorded before and after 58E02+ DAN activation that was either temporally paired or unpaired with KC stimulation. Dashed lines here and below represent >45-s delays.

(H) Representative γ4 MBON GCaMP responses to KC stimulation showing bidirectional modulation of KC-MBON signaling by activation of 58E02+ DANs depending upon whether DAN and KC activation were temporally paired or unpaired. Blue lines indicate time of KC stimulation.

(I) Changes in γ4 MBON responses to KC stimulation following activation of 58E02+ DANs that was either paired (left, n = 6, starting from a potentiated state) or unpaired (right, n = 12, starting from a depressed state) with KC stimulation are shown (see Figure S7 and Supplemental Experimental Procedures).

(J) Change in γ4 MBON response to an odor that was paired with 58E02+ DAN activation using $P2X_2$ relative to a second odor that was unpaired is shown (n = 10). All pairwise comparisons in this figure represent the mean (±SEM) with significant changes indicated as follows: *$p < 0.05$, **$p < 0.005$, and ***$p < 0.0005$.

See also Figure S7.